



## Measurements of reaction cross section with neutron and proton-rich radioactive beams

A.C.C. Villari, Wenlong Zhan, W. Mittig, G. Audi, L. Bianchi, A. Cunsolo, B. Fernandez, A. Foti, J. Gastebois, A. Gillibert, et al.

### ► To cite this version:

A.C.C. Villari, Wenlong Zhan, W. Mittig, G. Audi, L. Bianchi, et al.. Measurements of reaction cross section with neutron and proton-rich radioactive beams. International Winter Meeting on Nuclear Physics 27, Jan 1989, Bormio, Italy. 69, pp.74-85, 1989. <in2p3-00014476>

**HAL Id: in2p3-00014476**

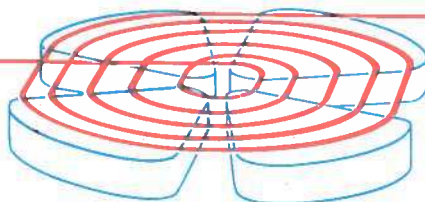
**<http://hal.in2p3.fr/in2p3-00014476>**

Submitted on 17 Apr 2014

**HAL** is a multi-disciplinary open access archive for the deposit and dissemination of scientific research documents, whether they are published or not. The documents may come from teaching and research institutions in France or abroad, or from public or private research centers.

L'archive ouverte pluridisciplinaire **HAL**, est destinée au dépôt et à la diffusion de documents scientifiques de niveau recherche, publiés ou non, émanant des établissements d'enseignement et de recherche français ou étrangers, des laboratoires publics ou privés.

# GANIL



**MEASUREMENTS OF REACTION CROSS SECTION  
WITH NEUTRON AND PROTON-RICH  
RADIOACTIVE BEAMS<sup>1)</sup>**

A.C.C. VILLARI<sup>a)</sup> - ZHAN WENLONG<sup>b)</sup> - W. MITTIG<sup>c)</sup> - G. AUDI<sup>d)</sup> -  
L. BIANCHI<sup>e)</sup> - A. CUNSOLO<sup>f)</sup> - B. FERNANDEZ<sup>e)</sup> - A. FOTI<sup>f)</sup> -  
J. GASTEBOIS<sup>e)</sup> - A. GILLIBERT<sup>e)</sup> - E. PLAGNOL<sup>c)</sup> - Y. SCHUTZ<sup>c)</sup> -  
C. STEPHAN<sup>d)</sup> and L. TASSAN-GOT<sup>d)</sup>.

- a) I.F.US.P. and CNPq, Sao Paulo, Brasil  
Present address : GANIL, B.P. 5027, F-14021 Caen (France)
- b) Institut of Modern Physics, Lanshou, China
- c) GANIL - Caen (France)
- d) Université de Paris-Sud, Orsay (France)
- e) DPhN-Saclay (France)
- f) I.N.F.N. Catania (Italy)

BORMIO XXVII (1989)

GANIL P89 06

# MEASUREMENTS OF REACTION CROSS SECTION WITH NEUTRON AND PROTON-RICH RADIOACTIVE BEAMS<sup>1)</sup>

A.C.C. Villari<sup>a)</sup>, Zhan Wenlong<sup>b)</sup>, W. Mittig<sup>c)</sup>, G. Audi<sup>d)</sup>, L. Bianchi<sup>e)</sup>,  
A. Cunsolo<sup>f)</sup>, B. Fernandez<sup>e)</sup>, A. Foti<sup>f)</sup>, J. Gastebois<sup>e)</sup>, A. Gillibert<sup>e)</sup>,  
E. Plagnol<sup>c)</sup>, Y. Schutz<sup>c)</sup>, C. Stephan<sup>d)</sup> and L. Tassan-Got<sup>d)</sup>.

- a) I.F.U.S.P. and CNPq, Sao Paulo, Brasil;  
Present address: GANIL, B.P.5027, F-14021 Caen (France)
- b) Institut of Modern Physics, Lanzhou, China
- c) GANIL - Caen (France)
- d) Université de Paris-Sud, Orsay (France)
- e) DPhN-Saclay (France)
- f) I.N.F.N., Catania (Italy)

## Abstract

The total energy integrated reaction cross section  $\sigma_R$  in the interaction of neutron and proton rich nuclei  $Z = 2 \sim 13$  secondary beam, produced at GANIL facility, with a thick Si or Cu target have been measured by detecting the associated  $\gamma$ -rays. The reduced strong absorption radius  $r_0^2$  which is proportional to the reaction cross section is calculated using a phenomenological parametrization that reproduces very well  $\sigma_R$  for stable nuclei. Comparisons between all results of different experiments, even by different groups are in agreement if only the associated  $\gamma$ -radiation is taken into account. The possibility of an experimental bias on this method is discussed. The behavior of  $r_0^2$  as function of  $(N-Z)$  reveals a predominance of shell effects. An enhancement of  $r_0^2$  for both neutron and proton rich regions is observed.

## I. Introduction

It may be expected that the structure of exotic nuclei, i.e. nuclei far from stability, would lead to new features of the nuclear matter. From this point of view, the study of nuclear reactions induced by exotic nuclei appears very interesting in order to test and to extend nuclear structure and reaction mechanism theories. Recently, secondary radioactive nuclei beams produced through projectile fragmentation at high and intermediate energies became available, opening the possibility to investigate this domain.

The total reaction cross section  $\sigma_R$  for the interaction of 790 A.MeV  ${}^3\text{He}$ ,  ${}^6,8\text{Li}$ ,  ${}^6,9,11\text{Li}$ ,  ${}^7,9\text{Be}$  and  ${}^8,12\text{Be}$  isotopes on Be, C and Al targets have been measured by Tanihata et al. [1]. An important deviation of the interaction radius, obtained from  $\sigma_R$ , when compared with Hartree-Fock-like calculations was observed for the very neutron rich nuclei  ${}^{11}\text{Li}$  and  ${}^{14}\text{Be}$ , that leads Tanihata et al. to suggest the existence of a large deformation and/or a long tail in the matter distribution of these nuclei [2].

---

1) Experiment performed at GANIL

Our previous results<sup>[3]</sup>, consisting of measurements of total reaction cross section of  $Z = 4 \sim 11$  neutron rich nuclei on Si indicated that  $\sigma_R$  increases with neutron excess faster than a  $(A_p^{1/3} + A_t^{1/3})$  law or than the phenomenological approach of Kox et al.<sup>[4]</sup>, that reproduces very well the existing experimental data of  $\sigma_R$  for several stable systems over a wide energy range.

Nevertheless, M.G. Saint-Laurent et al. claimed the non-observation of this enhancement in a similar experiment<sup>[5]</sup>.

In this contribution we present new experimental results for atomic numbers  $2 \leq Z \leq 13$  and for proton-rich as well as neutron-rich nuclei. We compare our results with all data obtained at this moment in the picture of the Kox relation.

## II. The method of associated $\gamma$ -rays and the energy-integrated reaction cross section

Our goal is to obtain the reaction cross section using a very low intensity radioactive beam. For the very exotic nuclei like  $^9\text{C}$  or  $^{20}\text{N}$  the production rate is around 10 counts per minute, which strongly limits the method and the quantities that can be measured. In order to increase the probability of reaction, we measure the energy-integrated reaction cross section. As we stop the beam in the target, the quantity measured can be written as follows :

$$\bar{\sigma}_R = \frac{1}{R} \int_{E_{\max}}^{\infty} \sigma_R(E) \cdot \frac{dR}{dE} dE \quad (1)$$

where  $R$  is the range of the incident particle in the target.

The technique is the associated  $\gamma$ -ray discussed by Bruandet<sup>[6]</sup>. The experimental device is shown in fig. 1. Secondary beams were produced as described in ref. 3 and 7 and transported up to the focal plane of the magnetic spectrograph SPEG at GANIL Laboratory. A telescope of two Si-surface barrier detectors of  $50 \mu\text{m}$  ( $\Delta E$ ) was used for Z-identification. Time of flight together with  $B_p$  and  $Z$  give an unique identification of all incident particles as shown in fig. 2. A detector array consisting of 16 hexagonal NaI(Tl) detectors  $13.1 \text{ cm}$  large and  $23.5 \text{ cm}$  long covering nearly  $4\pi$  surrounded the target of Si or Cu. The  $\gamma$ -detection efficiency for a single photon was 73 %. This arrangement essentially detected the associated  $\gamma$ -rays and, with lower probability, neutrons. The reaction probability  $P_{\text{reac}}$  was obtained by the number of coincidences between  $\Delta E$  and one or more of the  $\gamma$ -detectors divided by the total number of events in  $\Delta E$ . The relation between  $P_{\text{reac}}$  and  $\sigma_R$  can be expressed by :

$$\bar{\sigma}_R = \frac{-M_t \cdot \text{Log}(1 - P_{\text{reac}})}{N_A R} \quad (2)$$

where  $M_t$  is the target mass given in u and  $N_A$  is the Avogadro number.

In order to get informations on the nuclear properties of the involved exotic nuclei, it is necessary to extract an energy independent parameter. Such is the reduced strong absorption radius,  $r_0$ , in accordance with relationship :

$$\sigma_R(E) = \pi \cdot r_0^2 \cdot f(E) \quad (3)$$

Using for the function  $f(E)$  the Kox et al. parametrization<sup>[4]</sup>, we have :

$$\sigma_R(E) = \pi r_0^2 \cdot \left( A_p^{1/3} + A_t^{1/3} + a \cdot \frac{A_p^{1/3} \cdot A_t^{1/3}}{A_p^{1/3} + A_t^{1/3}} - C(E) \right)^2 \cdot \left( 1 - \frac{V_{cb}}{E_{CM}} \right) \quad (4)$$

where  $A_p$  and  $A_t$  are the projectile and target mass numbers,  $a = 1.85$  is an asymmetry parameter,  $c(E)$  is an energy dependent transparency and  $V_{cb}$  is the Coulomb barrier. The  $r_0^2$  should be independent of energy, target and projectile, as shown in ref. 4 for stable nuclei. The value of  $r_0^2$  in this case was found to be  $r_0^2 = 1.1 \text{ fm}^2$ . As an example of the meaning of  $\sigma_R$ , the reaction cross section for the system  $^{16}\text{O} + ^{28}\text{Si}$  at 41. A MeV incident energy, calculated using the relation (4) is drawn in Fig.3 as of function of the particle path in the Si target. With respect to the geometrical cross section, defined as the maximum  $\sigma_R$  obtained in this calculation, the transparency and Coulomb corrections are only 0.7% and 2.7% respectively. This feature supports the reliability of extracting accurate informations on the geometrical nuclear properties from the energy integrated cross section. In fact, we performed both corrections, assuming for the transparency  $C(E)$  the following linear dependence, valid up to about 100 A.MeV<sup>[8]</sup>:

$$C(E) = 0.31 + 0.0147 E/A_p \quad (5)$$

Our results are shown in terms of  $r_0^2$  and in function of the excess or deficiency of neutrons (N-Z). Neglecting higher order effects and adopting a stopping power approximation :

$$\frac{dE}{dR} \propto E^{-0.73}$$

we obtain from equations 2,3,4 and 5 :

$$r_0^2 = \frac{-M_t \cdot \text{Log}(1 - P_{\text{reac}})}{\pi R g^2 \cdot (1 - 2.37 V_{cb}/E_{CM} - 0.0147 E/A_p)} \quad (6)$$

where:

$$g = A_p^{1/3} + A_t^{1/3} + 1.85 \frac{A_p^{1/3} \cdot A_t^{1/3}}{A_p^{1/3} + A_t^{1/3}} - 0.31$$

One important problem in our measurements is the correction for efficiency of the detection system. We used a method different from ref. 5. We plot in Fig.4 the  $r_0^2$  values obtained for stable nuclei on both of the targets and for two different  $B_p$  values, that correspond to two different incident energies, as a function of the M-fold of the detection system. We see that all points fall on a smooth curve within an error of  $\pm 2\%$ .

The continuous and dashed lines are M-fold calculations supposing a primary exponential multiplicity distribution with a probability of emission of no  $\gamma$ -ray (dashed line) and without this component (continuous line). We can see that for low multiplicities, the probability of no  $\gamma$ -ray emission increases. However, it should be noted that, at least in first order, this effect can be rectified using the experimental efficiency correction. All raw experimental  $r_0^2$  obtained were corrected for efficiency

using the experimental curve of fig. 4.

The equation 6 was tested for different bombarding energies and targets. In fig. 5 we show for several isotopes of N, O, F and Ne,  $r_0^2$  obtained for three different Bp values, i.e. three different energies and over Si and Cu targets. We can see that all experimental points agree within the error bars. This result confirms the independence of  $r_0^2$  on the target nature and on energy, attesting the validity of eq. 4 and 6.

### III. Comparison between experiments

In our first experiment [3] the data analysis was performed in a different way from that described above. The information of  $\gamma$ -multiplicity could not be used directly because of a different set-up, a small NaI (T $\ell$ ) supplementary detector mounted very close to the target was used to detect both  $\gamma$ -rays and light particles ejected at forward angles. Supposing that the production of  $\gamma$ -rays and light particles are independent we can write :

$$\begin{aligned} N_{\gamma} &= P_{\gamma} \cdot N_R \\ N_{lp} &= P_{lp} \cdot N_R \\ N_{\gamma lp} &= P_{\gamma} \cdot P_{lp} \cdot N_R \end{aligned} \quad (7)$$

where  $N_{\gamma}$ ,  $N_{lp}$  and  $N_{\gamma lp}$  are the number of counts of  $\gamma$ -rays, light particles and  $\gamma$  and light particles in coincidence,  $P_{\gamma}$  and  $P_{lp}$  are the probabilities of detection of  $\gamma$  and light particles and  $N_R$  the number of reaction events.

Once we measured  $N_{\gamma}$ ,  $N_{lp}$  and  $N_{\gamma lp}$  we could obtain  $P_{\gamma}$ ,  $P_{lp}$  and  $N_R$ , that is proportional to  $\bar{\sigma}_R$  (eq. 2). It was observed that  $P_{lp}$  decreases as function of N-Z, but  $P_{\gamma}$  is constant within an error of 3 %. Using those informations we calculated an averaged efficiency correction of 27 % for the  $\gamma$ -detection system and obtained  $r_0^2$  using eq.6.

We reanalysed these data using the efficiency experimental curve of fig. 4 in order to compare the results of different experiments, all with the same method, i.e. the associated  $\gamma$  technique. The comparison between the results of the two analysis is shown in fig. 6. We can see two differences. First, the absolute value of  $r_0^2$  is smaller for the second analysis. Second, we can see a difference of slope of the data as function of N-Z. A 10 % difference of increase of  $r_0^2$  is observed. This difference can be understood by the fact that the first analysis takes into account the light particles produced in the reaction and determines an efficiency correction from equation 7, which takes into account unobserved reaction channels if the assumption of independence is correct. The second analysis only takes into account  $\gamma$ -rays. In order to stay consistent in the comparison of the results, we will use the second analysis of the data of ref. 5.

We compare our results with data of ref. 9 and with data of M.S. Saint-Laurent [7]. Having observed a discrepancy in absolute value of these two measurements in comparison with this work, we renormalised them by factors of 0.93 and 0.94 respectively. The comparison between all data is shown in fig. 7.

We can see that all experiments are in perfect agreement within the error bars for all nuclei where there is a superposition of data. Based on it, we calculated a weighed average of all existing data of associated- $\gamma$  technique and we present it in Fig. 8. In the same figure we compare our final results with those of Tanihata et al. [1] analysed with the same parametrization of eq. 4. Again we can see an almost perfect agreement between these results. Remark that for the case of  $^{11}\text{Li}$  the data of M.G. Saint-Laurent et al. and Tanihata et al. disagree by about 3 standard

deviations. Here we should note that the associated  $\gamma$ -ray technique can underestimate the reaction cross section and consequently  $r_0^2$  for the case of very neutron-rich nuclei. For these nuclei the break-up reaction leading to a nucleus in the ground state or at low excitation energy plus one or several neutrons is expected to increase significantly. Thus, the probability of emission of particles corresponding to a low detection efficiency and no  $\gamma$ -rays increases. Consequently, far from stability, the results presented using the associated  $\gamma$  technique should be confirmed by other experiments using different methods.

Nevertheless, all data reveal a strong influence of shell effects, for example the staggering effect in the data of Be and the strong structures in B and C. It is clear that these structures diminish in intensity moving to heavier systems like Ne or Na, as expected. Some effect of increasing of  $r_0^2$  for neutron rich nuclei can be seen for N and F. A strong enhancement, for the proton rich isotopes is seen for C.

In order to try to have a mean behaviour for all nuclei, independent of Z, we tried to calculate an averaged deviation  $\delta$  from the standard value  $r_0^2 = 1.1 \text{ fm}^2$  given by Kox. We added to all experimental data an artificial error of 5 % in order to try to wash out particular shell effects of each element Z. The final deviation  $\delta$  plotted in function of N-Z is showed in fig. 9. The shadowed zone represents the result and the error of a linear fit to both sides, neutron and proton-rich, supposing a  $|N-Z|$  dependence for  $r_0^2$ . We can see that an increase of  $r_0^2$  in function of  $|N-Z|$  is obtained. The mean effect is of order of 7% for  $N-Z = 10$ .

#### IV. Conclusions.

We measured the total-energy integrated reaction cross section  $\sigma_R$  in the interaction of neutron and proton-rich nuclei with  $2 \leq Z \leq 13$  secondary beams with a thick Si or Cu targets by detecting the associated  $\gamma$ -radiation. We calculated for all data obtained the reduced strong absorption radius  $r_0^2$  in the framework of Kox et al. parametrization. We compared our results with previous ones and those obtained by M.G. Saint-Laurent et al. and Tanihata et al. All results are in agreement over the whole range of elements. The behaviour of  $r_0^2$  as a function of the neutron or proton excess is predominantly governed by shell-effects. The average deviation  $\delta$  between all measured  $r_0^2$  with respect of a standard value  $r_0^2 = 1.1 \text{ fm}^2$  increases for both neutron and proton-rich regions. The magnitude of this effect is 7% for  $N-Z = 10$ . Note that this result is obtained using only the associated  $\gamma$ -radiation. It is about 10% smaller than we obtained using a determination of the  $\gamma$ -efficiency by the coincidences with charged particles. Either the assumption of independence of emission of  $\gamma$  and light particles used there does not hold or reaction channels where only neutrons are emitted contribute significantly. The disagreement for  $^{11}\text{Li}$  between the data of Tanihata et al. and the ones of M.G. Saint-Laurent et al. are compatible with the latter hypothesis. For the very neutron-rich region, the results obtained with the associated  $\gamma$ -technique may underestimate the total reaction cross section and should be checked by another method. Reactions leading to neutron break-up channels could play an important role far from stability. Measurements of these channels is desirable. Direct measurements of  $\sigma_R$  or elastic scattering data using exotic beams could also eliminate the remaining uncertainties.

### References.

- [1] I. Tanihata et al., Phys.Rev.Lett.55 (1985) 2676.  
I. Tanihata et al., Phys.Lett. 162B (1985) 217.  
I. Tanihata et al., Phys.Lett. 206B (1988) 592.
- [2] I. Tanihata, AIP Conference Proc., Nuclei far from Stability (1987).
- [3] W. Mittig et al., Phys.Rev.Lett. 59 (1987) 1889.
- [4] S. Kox et al., Phys. Rev. C35 (1987) 1678.
- [5] M.G. Saint-Laurent et al., 3rd Int. Conf. on Nucleus-Nucleus collisions, St. Malo, France (1988).
- [6] J.F. Bruandet, J. de Phys. C4 (1986) 125.
- [7] A. Gillibert et al., Phys.Lett. 176B (1986) 317.
- [8] B. Fernandez, private communication.
- [9] Zhan Wenlong et al., Nouvelles du Ganil, 21 (1987) 25.



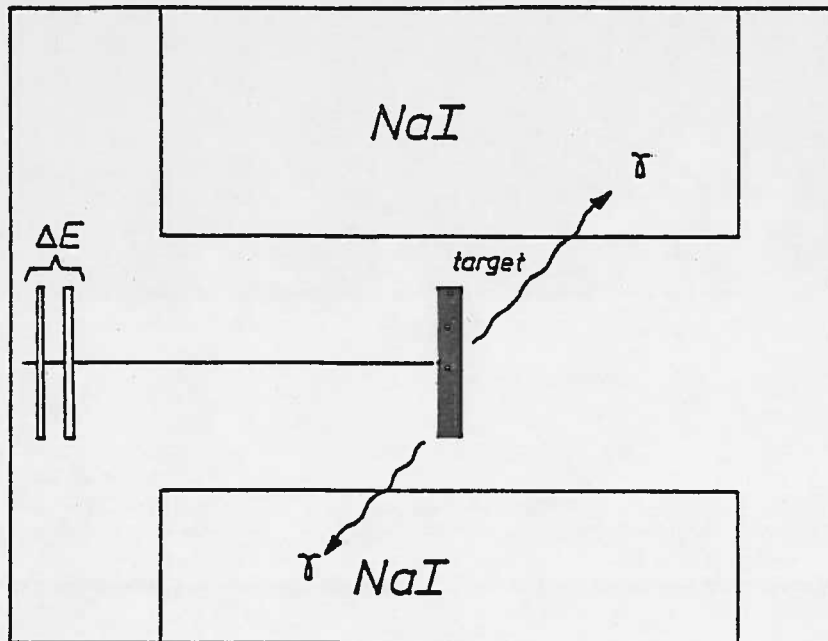


Fig.1) Experimental device for associated  $\gamma$ -radiation technique.

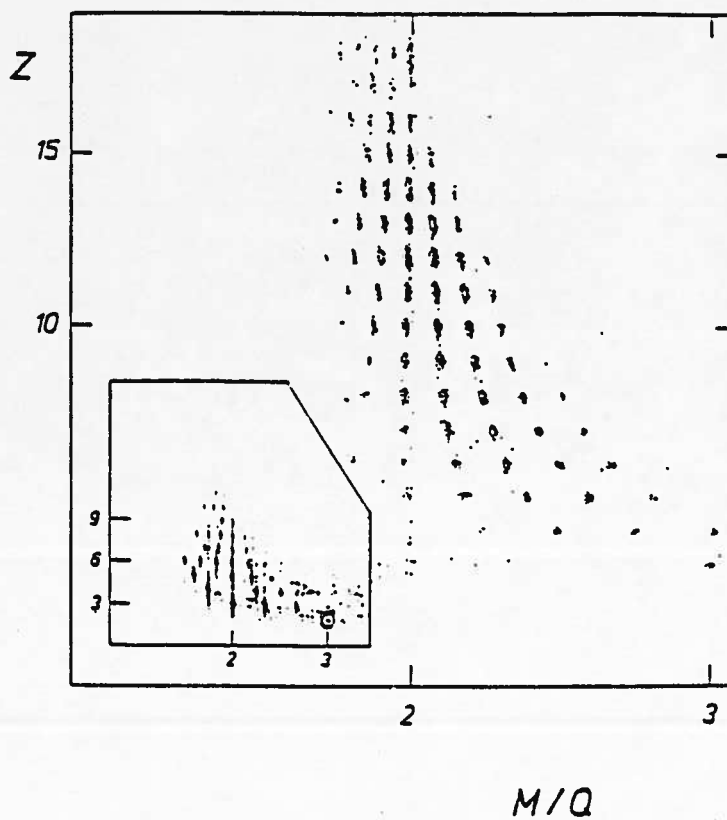


Fig.2) Matrix identification for two different  $B_p$  values.

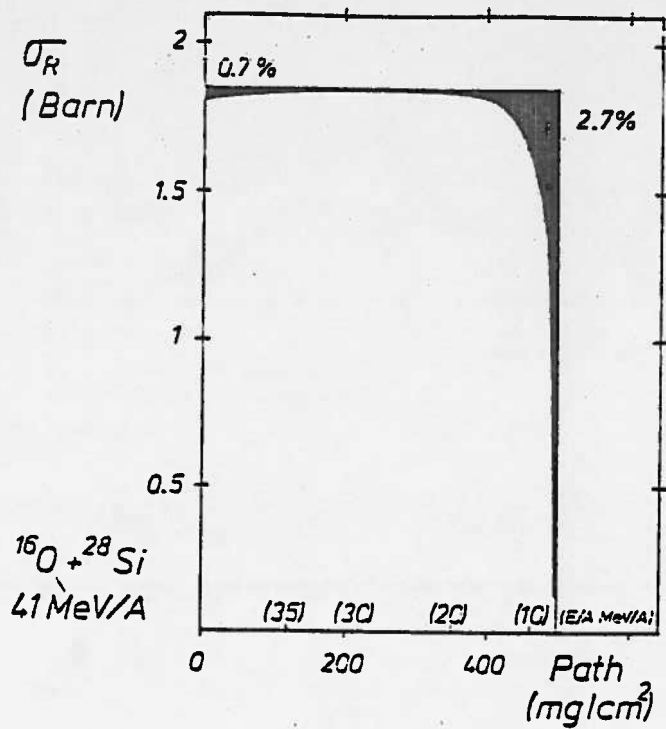


Fig.3)  $\sigma_R$  as a function of the particle path in the Si target calculated using eq.4. The black zones correspond to the effect of transparency (0.7%) and Coulomb correction (2.7%) with respect to the geometrical cross section.

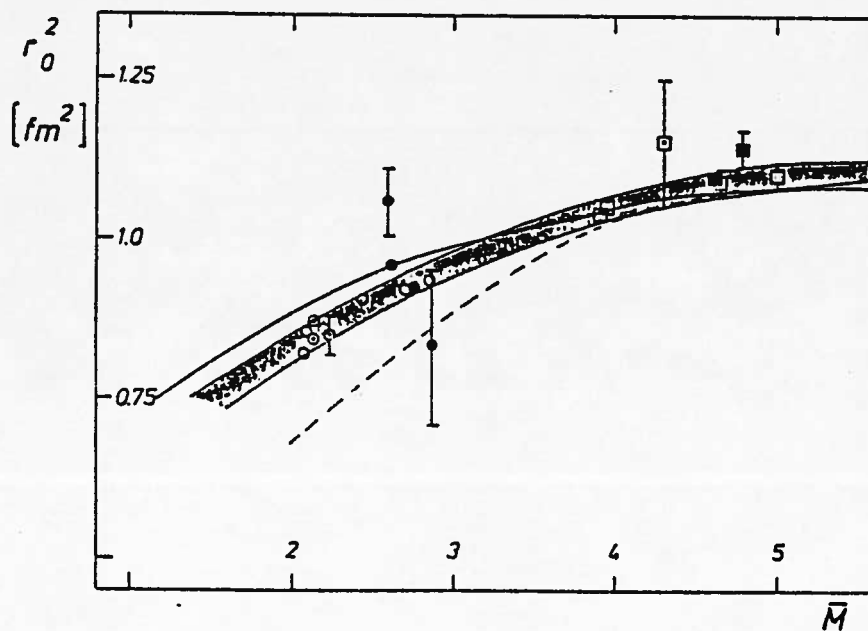


Fig.4) Experimental  $r_0^2$  as a function of  $\bar{M}$ -fold of the detection system for stable  $^{23}\text{Na}$ ,  $^{19}\text{F}$ ,  $^{15}\text{N}$ ,  $^{13}\text{C}$  and  $^{11}\text{B}$  projectiles for two magnetic rigidities  $B\rho = 1.877\text{Tm}$  (open symbols) and  $B\rho = 2.877\text{Tm}$  (Full symbols). The shadow zone drawn through the data points was used to correct the experimental data for efficiency. The dashed and continuous lines are Monte-Carlo calculations supposing an exponential primary multiplicity distribution with a probability of no emission of  $\gamma$ -ray and without this component respectively.

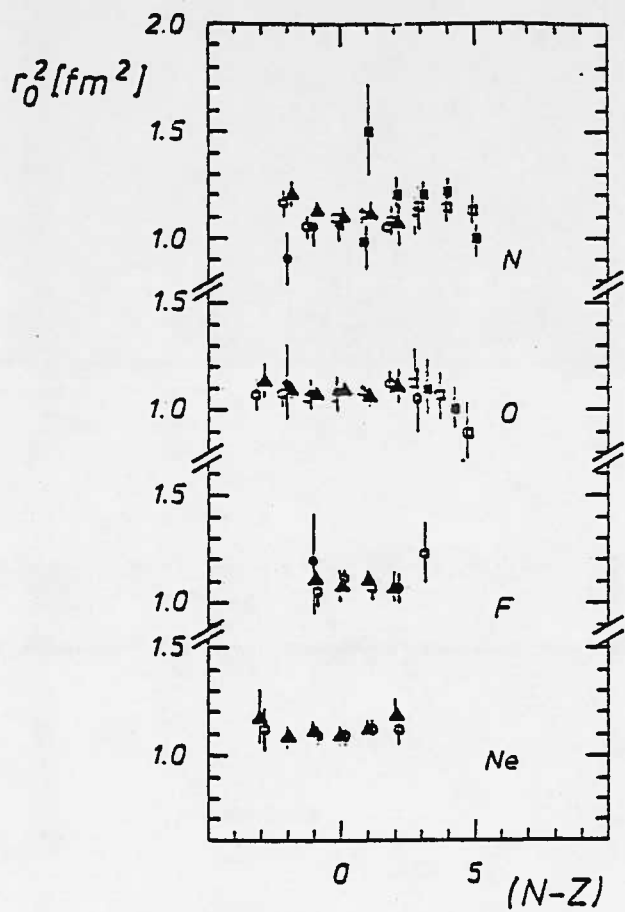


Fig.5)  $r_0^2$  obtained using different targets and magnetic rigidities

Target	$B\rho(\text{Tm})$	Symbol
Cu	2.877	■
Cu	1.870	▲
Si	2.877	□
Si	1.870	○
Si	1.391	●

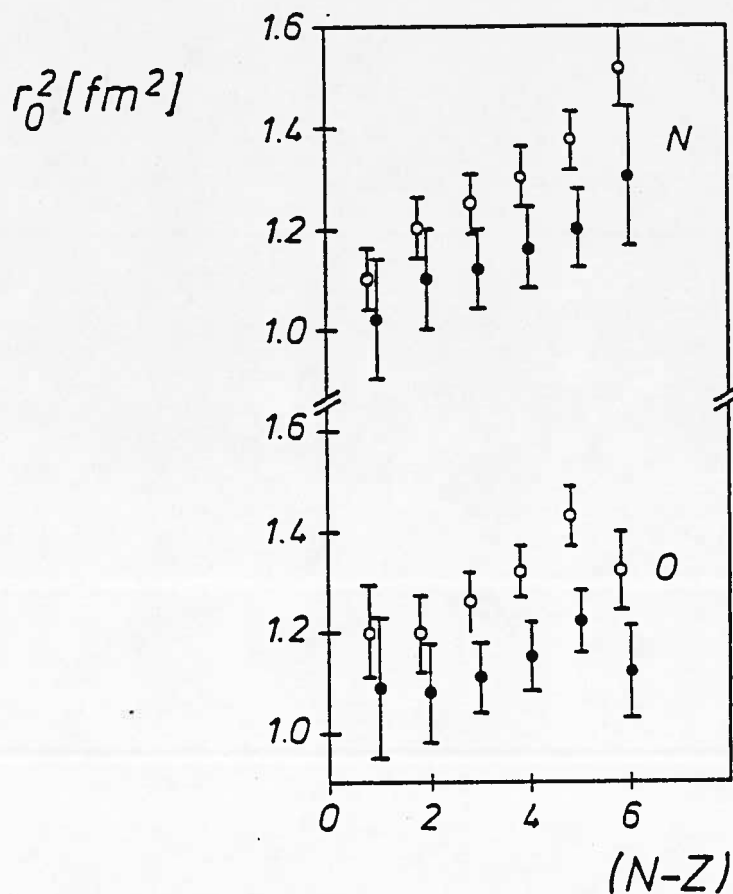


Fig.6) Comparison between original data of ref.3 (open points) with reanalysed ones (closed points).

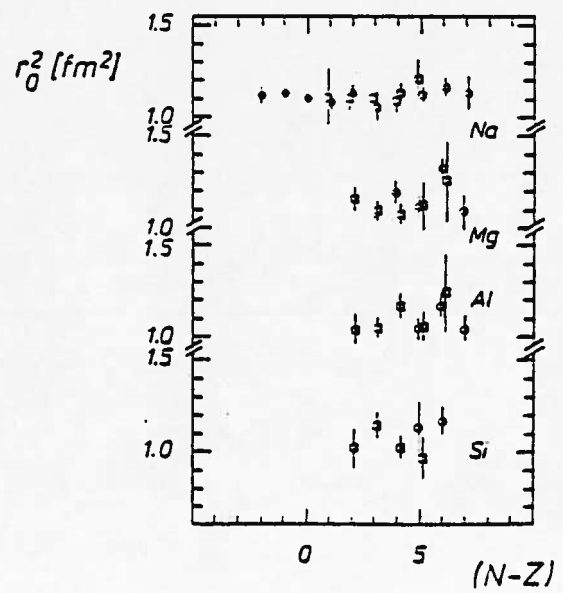
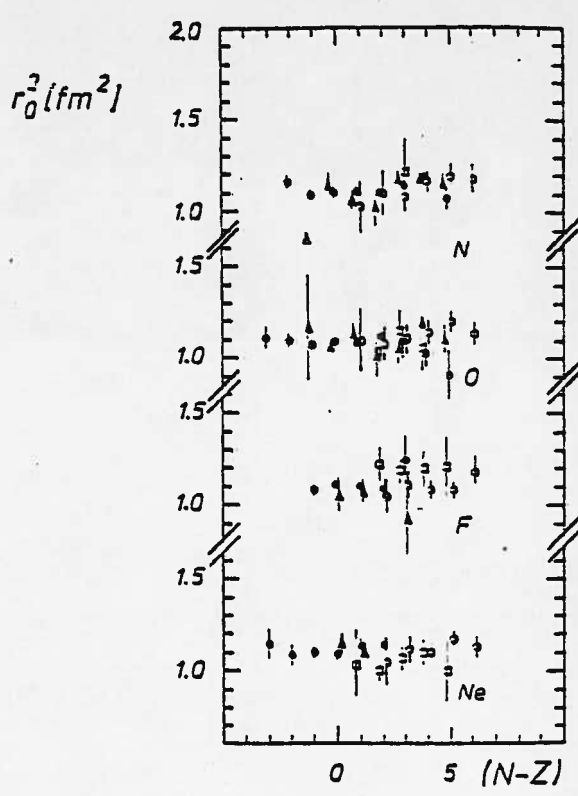
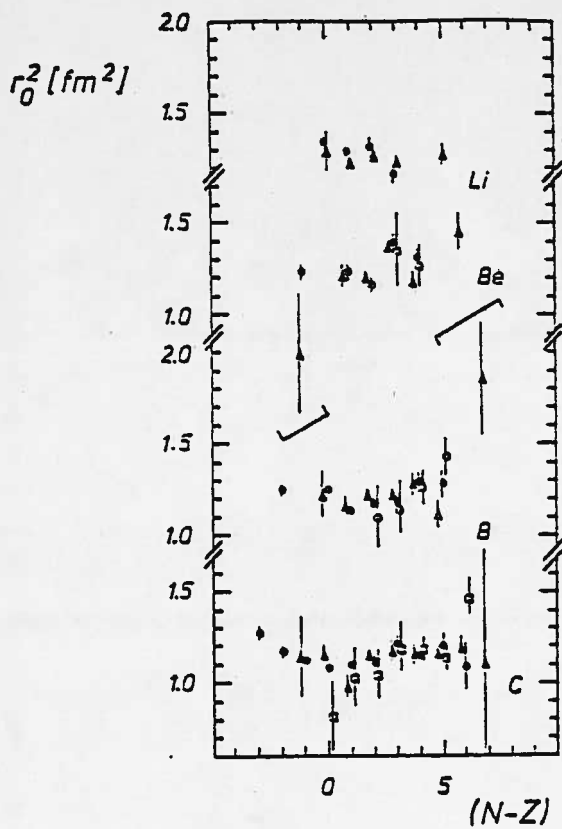
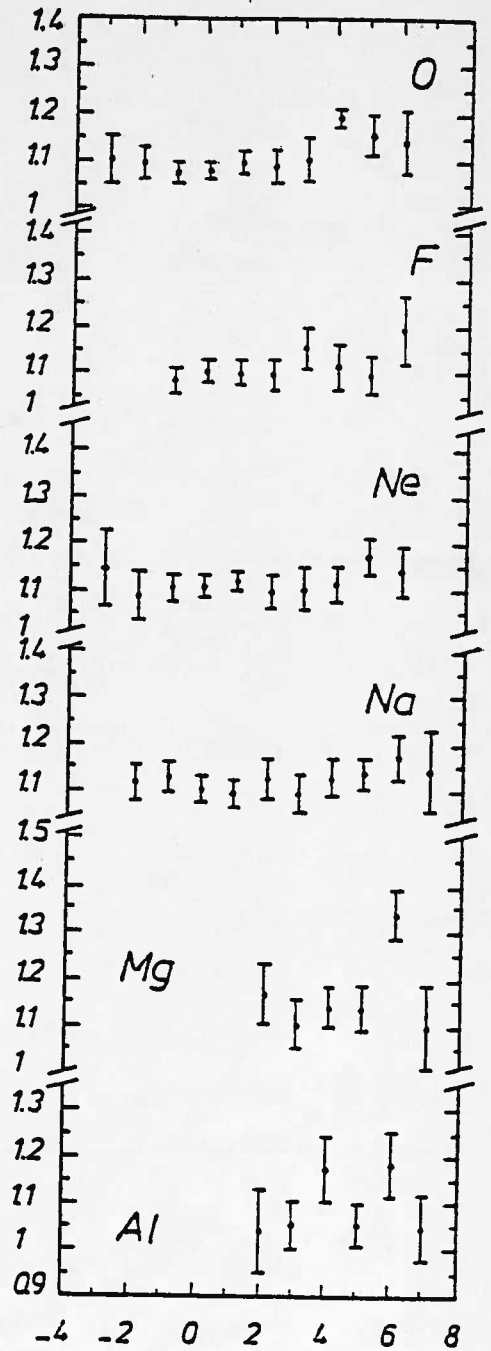
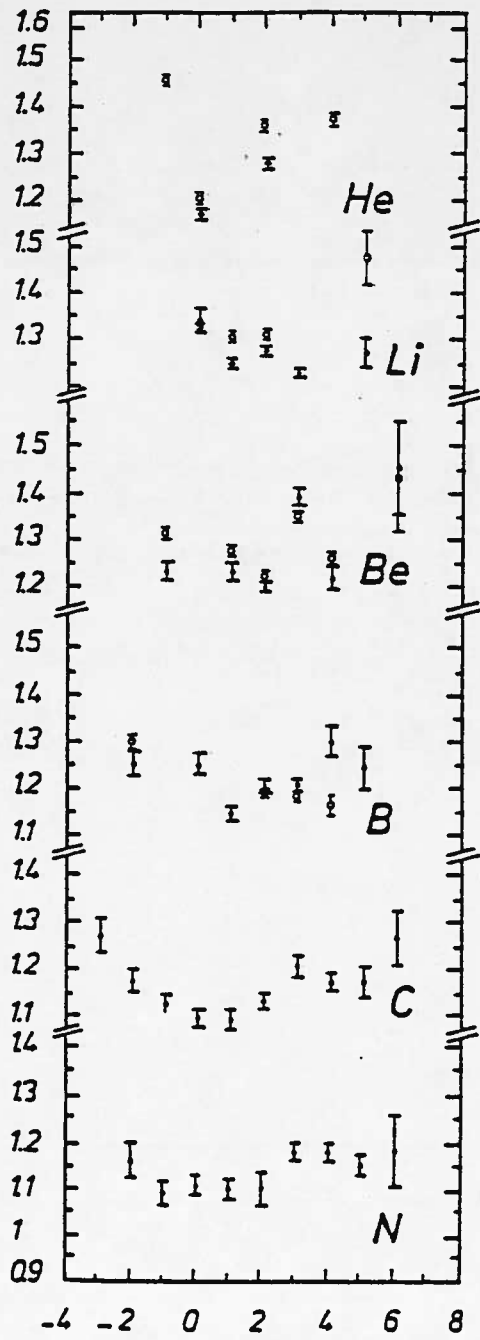


Fig.7) Comparison between all data of associated  $\gamma$ -radiation.  
 ● : this work  
 ○ : Ref.3 reanalysed  
 □ : Ref.9  
 ▲ : Ref.5

$r_0^2$  [fm<sup>2</sup>]



$(N-Z)$

Fig.8) Weighted averaged data for all isotopes (black points). Tanihata et al. data are the open circles.

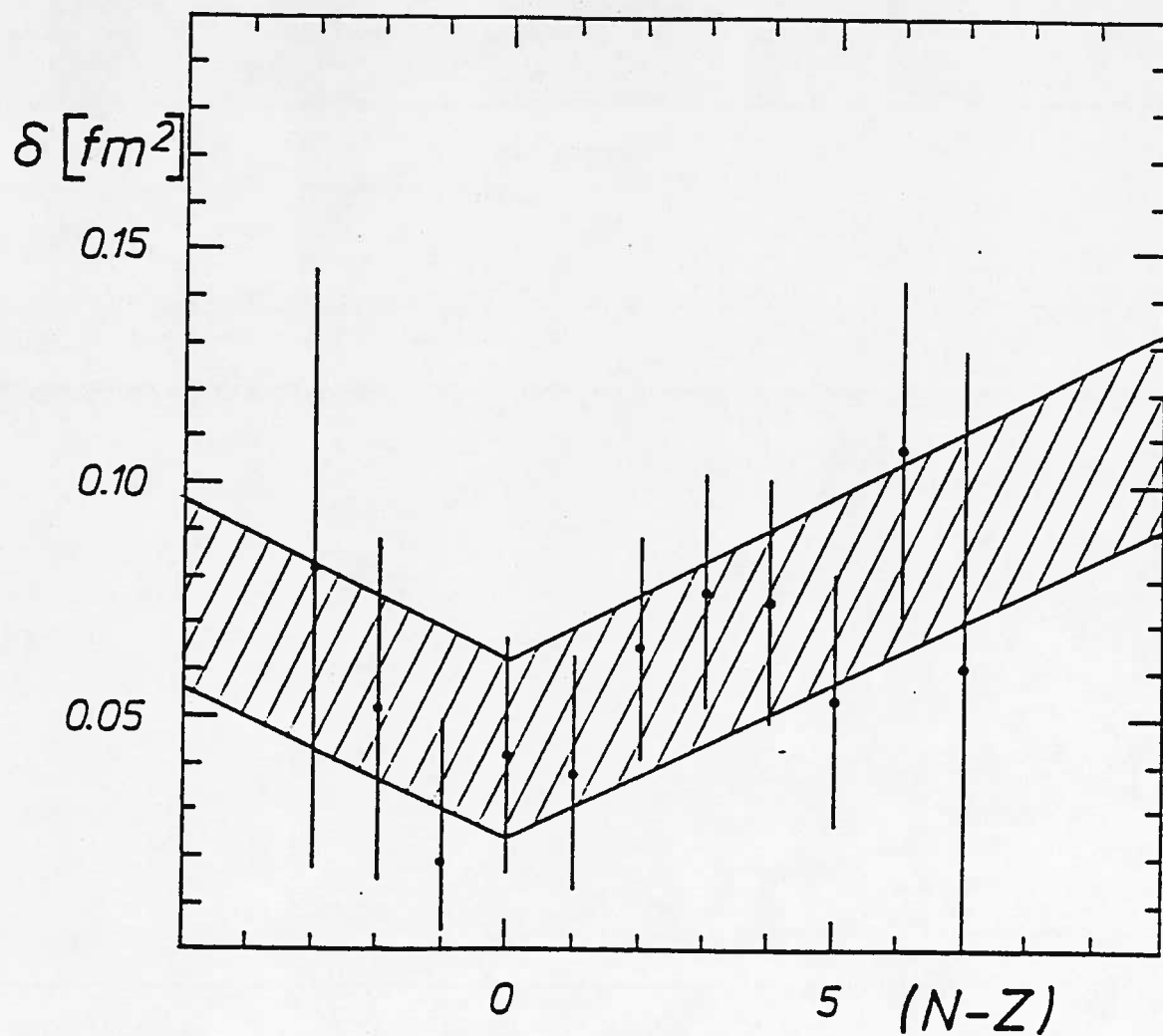


Fig.9) Average deviation  $\delta$  as a function of  $(N-Z)$ . The shadowed zone represents the result and the error of a linear fit to both sides, neutron and proton-rich, assuming a  $|N-Z|$  dependence for  $r_0^2$ .